Walther, S., Duveiller, G., Jung, M., Guanter, L., Cescatti, A., Camps-Valls, G. (2019): Satellite Observations of the Contrasting Response of Trees and Grasses to Variations in Water Availability. - *Geophysical Research Letters*, *46*, 3, pp. 1429—1440.

DOI: http://doi.org/10.1029/2018GL080535

Geophysical Research Letters

RESEARCH LETTER
10.1029/2018GL080535

Satellite Observations of the Contrasting Response of Trees and Grasses to Variations in Water Availability

Sophia Walther[1,2,3], Gregory Duveiller[2], Martin Jung[3], Luis Guanter[1,4], Alessandro Cescatti[2], and Gustau Camps-Valls[5]

[1]Helmholtz Centre Potsdam – GFZ German Research Centre for Geosciences, Potsdam, Germany, [2]Joint Research Centre, European Commission, Ispra, Italy, [3]Max-Planck-Institute for Biogeochemistry, Jena, Germany, [4]Institute of Earth and Environmental Science, Potsdam University, Potsdam, Germany, [5]Image Processing Laboratory (IPL), Universitat de València, València, Spain

Key Points:
- Satellite-based plant greenness, chlorophyll fluorescence, and gross photosynthesis are evaluated with respect to soil moisture fluctuations
- Ecosystem responses to water availability change sign along a tree cover gradient
- We show spaceborne observations of light- and temperature-enhanced forest photosynthesis in times of reduced soil moisture at constant greenness

Supporting Information:
- Supporting Information S1

Correspondence to:
S. Walther,
sophia.walther@bgc-jena.mpg.de

Citation:
Walther, S., Duveiller, G., Jung, M., Guanter, L., Cescatti, A., & Camps-Valls, G. (2019). Satellite observations of the contrasting response of trees and grasses to variations in water availability, *Geophysical Research Letters*, *46*, 1429–1440. https://doi.org/10.1029/2018GL080535

Received 12 OCT 2018
Accepted 18 JAN 2019
Accepted article online 25 JAN 2019
Published online 10 FEB 2019

Abstract Interannual variations in ecosystem primary productivity are dominated by water availability. Until recently, characterizing the photosynthetic response of different ecosystems to soil moisture anomalies was hampered by observational limitations. Here, we use a number of satellite-based proxies for productivity, including spectral indices, sun-induced chlorophyll fluorescence, and data-driven estimates of gross primary production, to reevaluate the relationship between terrestrial photosynthesis and water. In contrast to nonwoody vegetation, we find a resilience of forested ecosystems to reduced soil moisture. Sun-induced chlorophyll fluorescence and data-driven gross primary production indicate an increase in photosynthesis as a result of the accompanying higher amounts of light and temperature despite lowered light-use-efficiency. Conversely, remote sensing indicators of greenness reach their detection limit and largely remain stable. Our study thus highlights the differential responses of ecosystems along a tree cover gradient and illustrates the importance of differentiating photosynthesis indicators from those of greenness for the monitoring and understanding of ecosystems.

Plain Language Summary The capacity of vegetation to thrive and to sequester carbon depends on how much water they can have access to. In this work, we evaluate how different types of satellite observations can describe the response of vegetation to changes in soil moisture over the entire planet. The first source of observation measures only the greenness of the land surface, the second measures light that is emitted by pigments in plants which are photosynthetically active (chlorophyll fluorescence), and the third are simulations of gross carbon uptake derived from machine learning techniques. For periods of water shortage all three indicate a reduction of growth in ecosystems with few trees. However, in cold boreal forests, when soil moisture is particularly low, we still detect an increase in photosynthesis due to higher light and temperature conditions, but this is not reflected in the greenness indicator. This work illustrates how lack of water is not necessarily harmful for catching carbon through photosynthesis, but to monitor this effect, we need remote sensing indicators that measure more than just how green the plants are, and fluorescence is likely a good candidate.

1. Introduction

Several recent studies stress the dominant role of water availability in driving the interannual variability of photosynthetic activity and land carbon uptake at the global scale (Jung et al., 2011, 2017; Poulter et al., 2014; Vicente-Serrano et al., 2013). Water deficit has been reported to cause major reductions in photosynthesis (Barber et al., 2000; Barr et al., 2002; Ciais et al., 2005; Peng et al., 2011; Schwalm et al., 2012; Sun et al., 2015; Yoshida et al., 2015; Zscheischler et al., 2014), particularly in semiarid regions (Ahlström et al., 2015; Huang et al., 2016). Anomalies in precipitation caused by strong phases of the El Niño/Southern Oscillation are associated with large variability in the land carbon uptake in the semiarid ecosystems (Poulter et al., 2014) and in the tropics (Liu et al., 2017). For tropical ecosystems in particular, there has been a long debate on the degree of water limitation on photosynthesis (Asner & Alencar, 2010; Brando et al., 2010; Guan et al., 2015; Huete et al., 2006; Morton et al., 2014; Myneni et al., 2007; Nemani et al., 2003; Saleska et al., 2007; Wu et al., 2018). Negative impacts of water deficit (and heat) on gross primary productivity (GPP) are also reported for temperate and boreal forests (Allen et al., 2010; Angert et al., 2005; Barr et al., 2002; le Maire et al., 2010;

Peng et al., 2011; Piao et al., 2014; Sippel et al., 2017). However, neither the ecosystem strategies to cope with water stress (like the degree of isohydricity, enzymatic changes, carbon allocation, and structural changes of the canopy) nor the possible mechanisms overrunning drought resistance and resilience capacities (e.g., cavitation, carbon starvation, and critical soil moisture thresholds) are fully understood (Fisher et al., 2017; van der Molen et al., 2011). This is partly due to limited observational capabilities which only allow indirect diagnosis of terrestrial photosynthetic activity across large spatial domains.

Advances in satellite Earth observations from the last decades offer the means to systematically examine the state of vegetation structure and function at the proper spatial and temporal scales. Traditionally, this is done using vegetation indices based on red and near-infrared reflectances, such as the enhanced vegetation index (EVI; Huete et al., 2002), which serve as proxies for photosynthetic potential and relate to plant structure and chlorophyll content (i.e., green biomass). However, such indices will not respond to variations in water availability if these do not generate a marked change in green biomass. Estimations of GPP from flux tower eddy-covariance measurements do capture such water stress-related variations in photosynthesis that occur in the absence of changes in greenness, but they are only available over few unevenly distributed sites (Schimel et al., 2015). This has resulted in efforts to generate spatially explicit simulations of GPP by training machine learning algorithms to upscale site-level empirical relationships between flux tower GPP and environmental and land surface properties derived from satellite observations (Beer et al., 2010; Jung et al., 2011; Tramontana et al., 2016). In parallel, a new possibility for estimating GPP directly from space at global scale has emerged using sun-induced chlorophyll fluorescence (SIF). SIF is a weak electromagnetic signal emitted by photosynthesising plants driven by the amount of radiation absorbed by chlorophyll (APAR). SIF also contains information on the efficiency with which the absorbed energy is used in carbon assimilation through the fraction of absorbed light that is reemitted as SIF (Frankenberg et al., 2011; Joiner et al., 2011; Meroni et al., 2009; Porcar-Castell et al., 2014; Yoshida et al., 2015; Zarco-Tejada et al., 2013). Similar to a model describing GPP after Monteith (1972), SIF can be formalized as

$$SIF = APAR * LUEf * f_{esc} \quad (1)$$

where LUEf describes the light-use-efficiency of fluorescence and f_{esc} the escape probability of a SIF photon from the canopy due to scattering and reabsorption. However, the respective contributions of the factors in equation (1) to the total SIF signal across time still need to be disentangled, while further research is also needed to understand the explicit coupling of SIF to GPP over these scales (Porcar-Castell et al., 2014).

Given the importance of both GPP and water availability for land carbon uptake, we analyze how productivity varies with both positive and negative anomaly events in soil moisture content of various intensities in global ecosystems along a tree cover gradient. Our assessment is based on a simultaneous evaluation of all three indicators: estimated GPP, SIF, and EVI.

2. Data and Methods

2.1. Data

We use data sets aggregated to 16 days (sampled every 8 days) and to 1° from their native resolution, which minimizes noise and is sufficient to investigate the global patterns in temporal variability of vegetation primary productivity and its relation to climate drivers. However, for the analysis of the effect of tree cover on the vegetation response to changes in soil water a finer spatial resolution is more meaningful and we use 0.5° data. The study period comprises the years from 2007 to 2015.

2.1.1. SIF

The longest available SIF data records (from January 2007 onward) originate from measurements of the GOME-2 instrument onboard the MetOp-A satellite. Based on the GOME-2 observations, global far-red SIF data sets (740 nm) have been produced (Köhler et al., 2015, ungridded level 2 data). From the individual measurements those taken under sun zenith angles larger than 70°, after 2 p.m. or before 8 a.m. local solar time were excluded. In order to remove the data with the highest cloud contamination, the effective cloud fraction was used to filter out observations with cloud fractions larger than 50%. The remaining valid observations were gridded to 1° spatial and 16 days temporal resolution.

2.1.2. Greenness Indices and Land Cover

The greenness index EVI (Huete et al., 2002) has been calculated from Moderate Resolution Imaging Spectroradiometer (MODIS) nadir surface reflectance measurements. MCD43C4v005 data were

retrieved from the online Reverb, courtesy of the National Aeronautics and Space Administration (NASA) EOSDIS Land Processes Distributed Active Archive Center, U.S. Geological Survey (USGS)/Earth Resources Observation and Science Center, Sioux Falls, South Dakota, https://lpdaac.usgs.gov/dataset_discovery/modis/modis_products_table/mcd43c4. The surface reflectances gridded at 0.05° have been filtered for snow and good quality retrievals (quality flags 0 and 1, meaning at least 75% with full or best inversions); the EVI has been calculated and then aggregated to 1° spatial resolution.

Furthermore, information on land cover according to the International Geosphere Biosphere Programme classification has been retrieved from the MCD12C1 file for 2009 (we take this year as representative for the whole study period) in order to exclude regions from the analysis that are covered by water and ice or that are barren. We aggregated it to 1° spatial resolution by assigning the land cover class with the most frequent occurrence in all subpixels of 0.05°.

2.1.3. Data-Driven GPP Model Simulations

Additional comparisons are carried out with model results of GPP from the FLUXCOM simulations (Tramontana et al., 2016, http://www.fluxcom.org/products.html). Different machine learning techniques are used to spatially upscale the empirical relationship established at FLUXNET eddy-covariance tower locations between GPP and various land surface variables to the globe (we use the FLUXCOM-RS setup where only remotely sensed variables inferred from MODIS measurements are used as explanatory variables). We use the median of an ensemble of 18 simulations that come with a native resolution of 1/12° and 8 days.

2.1.4. Meteorological Data and Soil Water Content

To study the environmental effects on vegetation, we look at temperature and water conditions using the air temperature at 2-m height and the volumetric soil water content in the four layers between 0- to 7-, 7- to 28-, 28- to 100-, and 100-to 289-cm depth from ERA-Interim reanalysis data (Dee et al., 2011). We convert the volumetric soil water content in cubic meters per cubic meters to millimeters and additionally take an average across all four soil layers weighted by the layer thickness.

In order to have an estimate of the incoming radiation, we use all-sky surface fluxes of downward shortwave radiation (global radiation) computed from observed top-of-atmosphere fluxes that are distributed at 1° spatial and daily temporal resolution (the "SYN1deg-Day product," Ed4A) by the Clouds and the Earth's Radiant Energy System (CERES) onboard of the Aqua and Terra satellites (Doelling et al., 2013). Disaggregation to 0.5° spatial resolution is accomplished by bilinear interpolation.

2.1.5. Tree Cover and Köppen Climate Classification

Information on the amount of tree cover is inferred from the global maps of forest cover gain and loss by Hansen et al. (2013) based on Landsat images. The global forest cover in 2009 (with tree cover defined as the areal coverage with canopies of more than 5-m height) has been obtained by combining information on the global tree cover in 2000 and the yearly losses until 2009. The gains until 2009 have been estimated from the given growth by 2012 assuming a linear growth between 2000 and 2012. This information on forest cover in 2009 has subsequently been aggregated from the native 30-arc sec resolution to 1°. Climate classification is based on the latest release of the global map of the Köppen-Geiger classification representative for the period 1986–2010 (Kottek et al., 2006; Rubel et al., 2017).

It is a known issue that SIF measurements suffer from noise contamination in South America due to high cosmic particle fluxes in the region of the South Atlantic Anomaly (Köhler et al., 2015). We therefore exclude this region (Transcom region 4, all of South America except larger Amazonia) from all analyses.

2.2. Methods

2.2.1. Normalized Deviations From the Average Behavior

All data streams of vegetation proxies and of meteorological and soil moisture conditions are treated in the same way in that first a linear trend is removed and subsequently the mean seasonal cycle is subtracted in each pixel. The resulting deviations from the average temporal behavior originate from shifts in phenology and will be a natural reaction of the vegetation to meteorological variations. They do not describe anomalous (in the sense of unexpected) behavior of the plants. The analysis of the deviations is limited to the growing season. See supporting information Text 2 for details on the data treatment (Baumbach et al., 2017; Braswell et al., 1997; Ceccherini et al., 2014; Donges et al., 2016; Frank et al., 2015; le Maire et al., 2010; Lyapustin et al., 2014; Mahecha et al., 2017; Moore et al., 2016; Rammig et al., 2015; Smith, 2011; Vicca et al., 2016; Wu et al., 2012; Zhang et al., 2016; Zhou et al., 2016; Zscheischler et al., 2013, 2014).

A standardization of each data set by its area weighted standard deviation across the whole data cube will make the deviations comparable between vegetation proxies as well as their ranges and units. In this procedure each voxel at the position x (longitude),y (latitude), t (time) in the cube of deviations is first weighted by the cosine of the latitude as an approximation of grid cell area.

$$\Delta\text{proxy}^{\text{weighted}}_{x,y,t} = \Delta\text{proxy}_{x,y,t} * \cos(\text{lat}(y)) \tag{2}$$

The normalized deviations are then defined as

$$\Delta\text{proxy}^{\text{norm}} = \frac{\Delta\text{proxy}}{\text{sd}(\Delta\text{proxy}^{\text{weighted}}_{1:n})} \tag{3}$$

where 1:n denotes all voxels in space and time.

Hence, the resulting deviations from the average vegetation behavior are measured in units of "global (spatiotemporal) standard deviations (global SD)."

2.2.2. Event-Based Analysis

The link between meteorology and vegetation variability is studied from a driver perspective, which means that we define events based on deviations from climatology in one meteorological variable. Then, the corresponding deviation in the vegetation proxies is analyzed for each meteorological event. We use deviations in the soil water content to define a meteorological event as consecutive 16-day periods (time steps) of positive (negative) deviations in a given pixel. We then sum the deviations of a given vegetation proxy in the same pixel x,y over the duration of a given event k and will obtain the integrated deviation (or event size) as the immediate vegetation response to the soil moisture event.

$$\text{event}^{\text{proxy}}_{x,y,k} = \sum_{i=t_m}^{t_n} \Delta proxy_{x,y,i} \tag{4}$$

where the first time step t_m and the last one t_n belonging to the event k are defined by the deviations in soil moisture

$$\Delta\text{SM}_{x,y,t_m \ldots t_n} > 0 \,\&\, \Delta SM_{x,y,t_m-1} < 0 \,\&\, \Delta\text{SM}_{x,y,t_n+1} < 0$$

or

$$\Delta\text{SM}_{x,y,t_m \ldots t_n} < 0 \,\&\, \Delta\text{SM}_{x,y,t_m-1} > 0 \,\&\, \Delta\text{SM}_{x,y,t_n+1} > 0$$

Iterating over all pixels and events, we will thus obtain integrated vegetation deviations that can be compared across proxies in a consistent way, since the meteorological events are the same for every vegetation proxy. For summary plots other than maps the deviations are weighted by their areal contributions to the average (again, a pixel value is weighted with the cosine of the latitude). For the soil moisture we show integrated event sizes of relative deviations in order to make deviations in soil moisture comparable across space. The relative deviations in soil moisture are defined as

$$\Delta\text{SM}^{\text{rel}}_{x,y,ts,a} = \frac{\Delta\text{SM}_{x,y,ts,a}}{\overline{\text{SM}_{x,y,ts}}} \tag{5}$$

with subscript ts denoting a time step of the year and a a given year.

3. Results

3.1. Contrasting Patterns of Vegetation Productivity Associated With Below Average Soil Water Content

A spatial diagnostic of the average vegetation deviation associated with periods of below average soil moisture illustrates how both photosynthesis (represented by SIF and model GPP) and greenness (EVI) strongly decrease in large parts of the world (Figure 1). These areas mainly correspond to semiarid regions where the vegetation cover is dominated by grassland, savannah and cropland, with little or no trees (Figure 1d). In such areas, vegetation activity heavily depends on water availability and is therefore highly variable (Ahlström et al., 2015; Poulter et al., 2014; cf. supporting information Figures S2 and S3), and strongly coupled to the atmosphere (Koster et al., 2004; Zscheischler et al., 2015). On the contrary, in ecosystems with

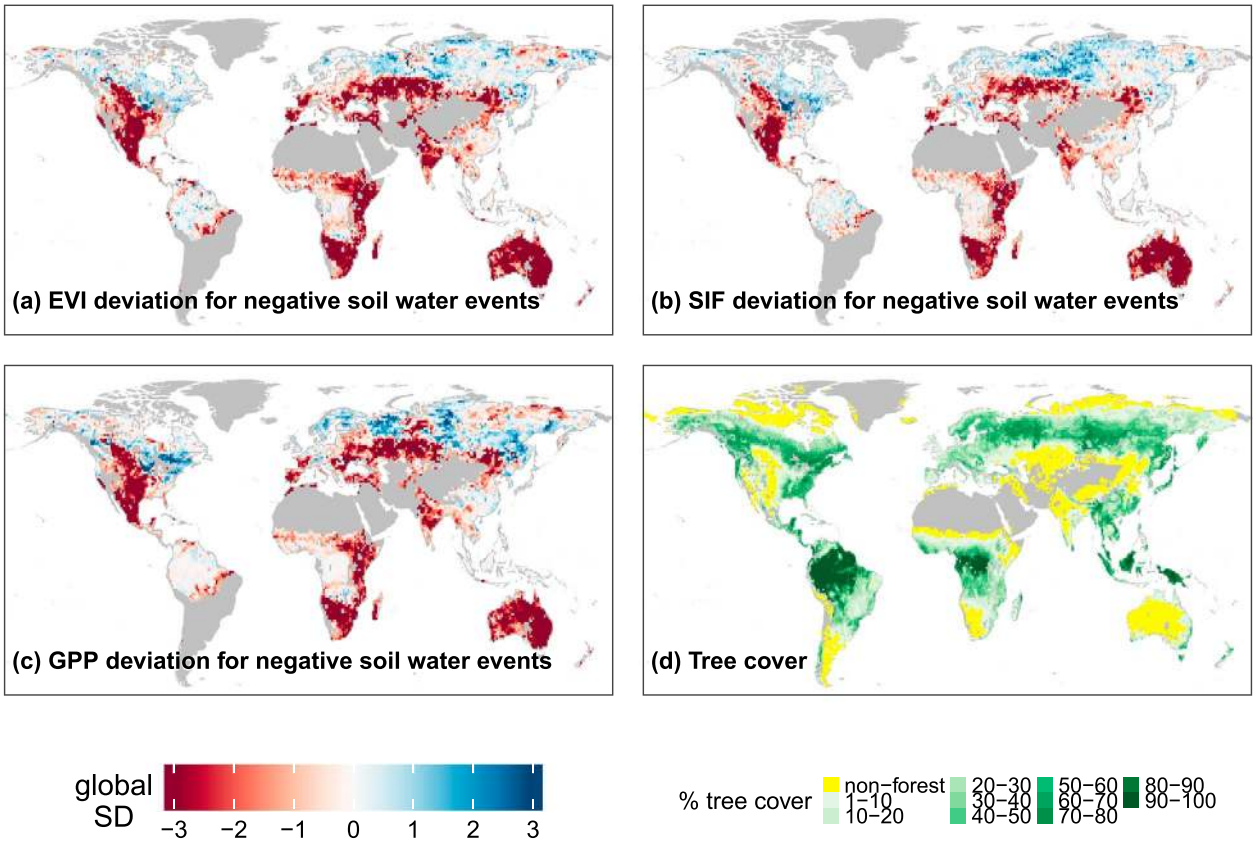

Figure 1. Typical vegetation reaction to below average soil water content: (a–c) deviations seen in the vegetation observations averaged across all events of reduced soil moisture. Units are given in "global SD," meaning the standard deviation in space and time across the data cube of deviations (see section 2.2). (d) Average amount of tree cover in a pixel. EVI = enhanced vegetation index; SIF = sun-induced chlorophyll fluorescence; GPP = gross primary productivity.

medium-to-high tree cover, results show a relative increase in photosynthesis in periods of reduced water availability. To better analyze this pattern, Figures 2a–2c display the deviations from the mean in productivity and greenness along a tree cover gradient and across a range of different intensities in anomalies in water availability. For nonforested ecosystems, the three vegetation proxies consistently show the expected synchronous patterns of reduced/increased photosynthesis and greenness in times of decreased/enhanced soil water content. Furthermore, the magnitude of the vegetation anomaly increases with the strength of the departure of soil moisture from the mean, as expected. The situation changes along the tree cover gradient as both SIF and modeled GPP detect a clear reversal in the sign of the deviations in photosynthesis co-occurring with strong anomalies in water content. Here, water deficits are actually associated with increased photosynthesis whereas wetter-than-usual periods lower it (cf. Figure S4). This effect is persistent even when considering soil moisture anomalies at different soil depths (supporting information Figure S5). These regional patterns of enhanced photosynthesis are in contrast to the established perception that reduced water availability has a generally negative impact on the primary productivity of terrestrial ecosystems (Liu et al., 2013; Reichstein et al., 2013; Schwalm et al., 2012; Zhao & Running, 2010). Interestingly, the traditional satellite-based greenness index (EVI) is not markedly enhanced in forests during periods of reduced soil moisture and has a different threshold of inversion along the tree cover gradient (cf. short discussion in supporting information Text S3).

We further decompose SIF and GPP into anomalies of absorbed radiation (APAR), here approximated as the product of EVI with radiation, and light-use-efficiency (LUEf and LUEp, SIF, or GPP divided by APAR, respectively; Figures 2d–2f; ; Monteith, 1972). The dominant pattern of deviations in the photosynthesis proxies is qualitatively consistent with APAR anomalies. This suggests that in periods of diminished soil moisture, more incoming light combined with weak changes in greenness drives the positive photosynthesis response in forests. Conversely, for ecosystems with low to moderate tree cover, negative deviations in APAR are largely due to strong declines in greenness. Consistent with theoretical expectations, LUE

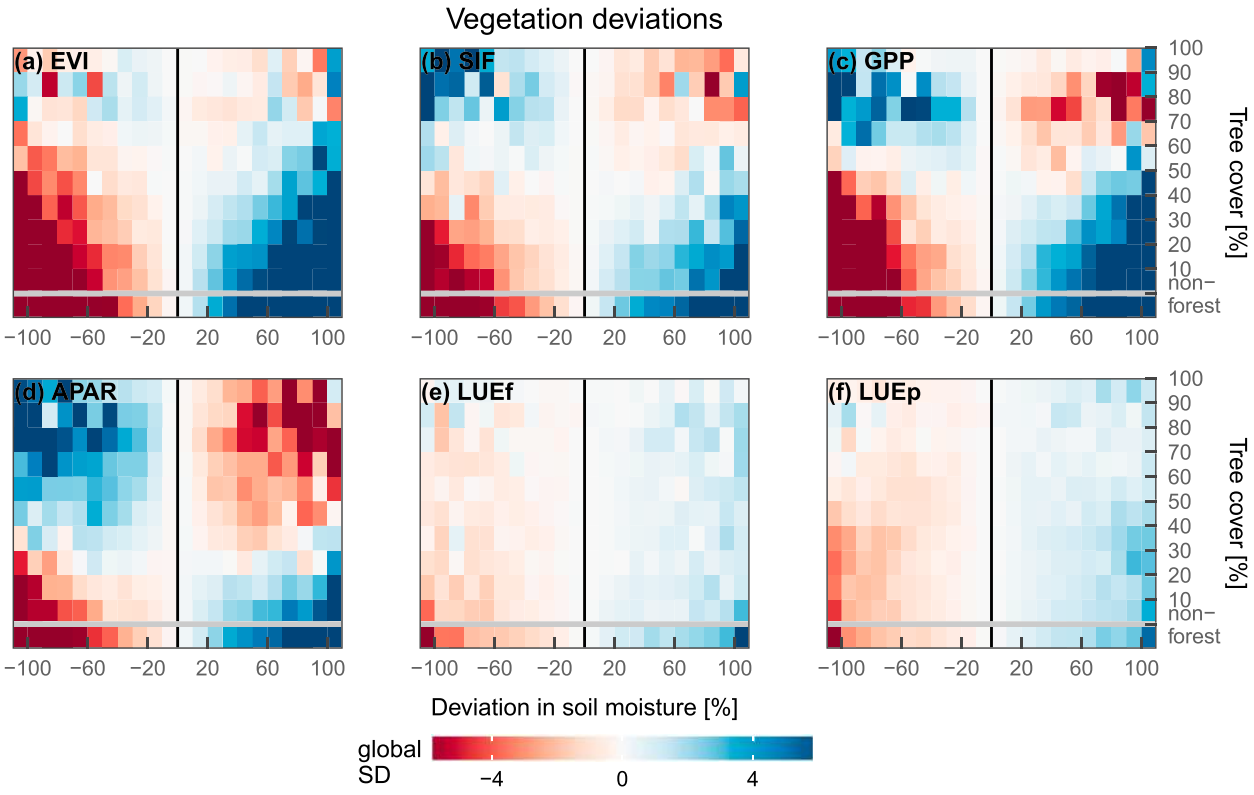

Figure 2. Patterns of vegetation greenness, photosynthesis, APAR, and LUE associated with water availability along a tree cover gradient: average deviation seen in the vegetation proxies for a given anomaly in the soil water content and as a function of the amount of trees in the given pixel. Nonforest is defined as ecosystems with a tree cover fraction of below 1%. APAR is approximated as $EVI * Rg$, fluorescence yield LUEf as $SIF/(EVI * Rg)$, and photosynthetic light-use-efficiency LUEp as $GPP/(EVI * Rg)$. EVI = enhanced vegetation index; SIF = sun-induced chlorophyll fluorescence; GPP = gross primary productivity; APAR = absorbed photosynthetically active radiation; LUE = light-use-efficiency; SD = standard deviation.

(LUEf and LUEp) is generally reduced when soil moisture is below average, also for forests. This suggests that the photosynthetic performance is decreased below maximum potential levels (which are dictated by APAR) due to colimiting effects of temperature and water on LUEp and further implies that SIF carries also information on physiological responses of photosynthesis beyond green APAR, which are detectable from space (Yoshida et al., 2015). Interestingly, the decline of LUE with soil moisture is weaker for forests compared to nonforests. This likely reflects reduced sensitivities of trees to depleted soil moisture due to deeper and more extensive root systems that facilitate larger access to available moisture. The combined effects of fluctuations in APAR and LUE shape photosynthesis anomaly patterns. In times of decreased soil water content, negative deviations in LUE amplify the effect of lowered APAR for low tree cover which results in the reduction of photosynthesis, while reduced LUE dampens the increased APAR for forests.

3.2. The Roles of Light, Climate, and Tree Density in Determining the Photosynthetic Response to Soil Moisture

To explore the mechanism behind the differential response of greenness and photosynthesis to altered water availability, we examine the covariation of temperature, incoming radiation and soil moisture with those vegetation proxies directly derived from satellite. Figure 3 presents the partial correlations in time of deviations in SIF and EVI with respect to either temperature, incoming radiation or soil moisture, whilst controlling for the remaining two. Soil moisture is the variable showing the largest partial correlations for both SIF and EVI in regions with low or no tree cover. This confirms that variations in soil water content affect nonforested ecosystems mainly by causing plant structural and pigment changes (i.e., chlorophyll content and leaf area; Zhang et al., 2016), which translate into the observed variability in greenness, photosynthesis and APAR. For intermediate fractions of tree cover, temperature contributes to explaining the temporal variations of both EVI and SIF, while the partial correlations with soil moisture decrease to 0. For dense forests, however, partial correlations of SIF and EVI with both soil moisture and temperature drop and radiation becomes the single-most important driver of variability in SIF, while EVI remains negatively correlated to radiation. This

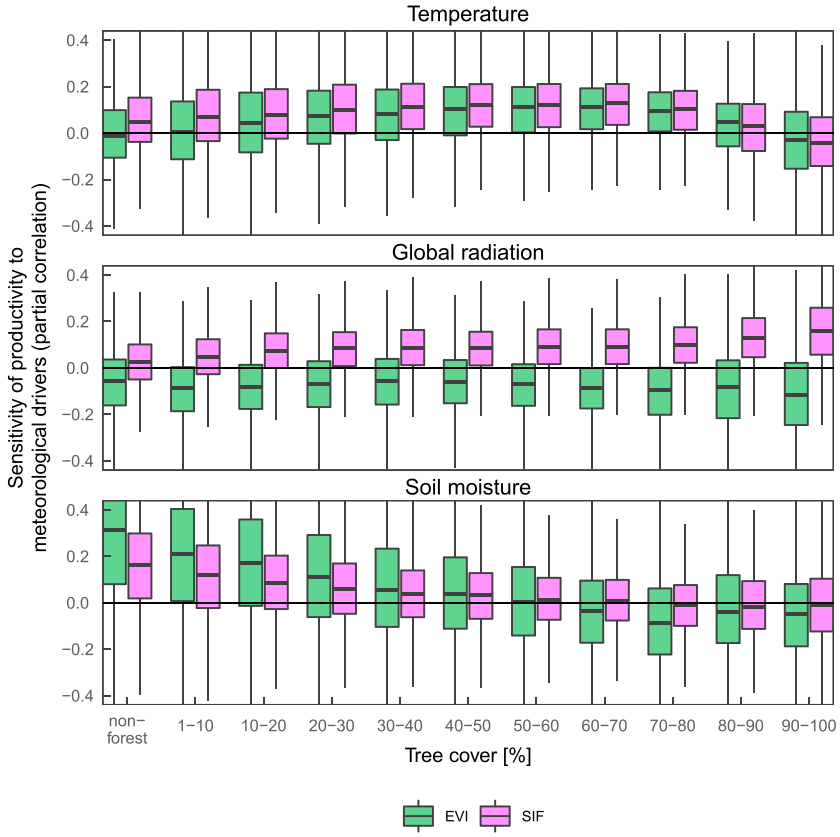

Figure 3. The strength of the relationship between vegetation greenness or photosynthesis and anomalies in meteorology for different amounts of tree cover: partial correlations in time between temporal fluctuations in vegetation proxies and global radiation, temperature, or soil moisture with the effects of the corresponding other two meteorological variables removed. Partial correlations are summarized as a function of tree coverage based here on 0.5° resolution data. EVI = enhanced vegetation index; SIF = sun-induced chlorophyll fluorescence.

pattern indicates that generally in forests, primary productivity is mainly controlled by incoming radiation and temperature, with light being the dominant factor in the most dense forests (cf. the consistent results for model GPP in supporting information Figure S6). The increase in photosynthesis also raises transpiration (Koirala et al., 2017), which would result in a reduction of soil water content that is less likely to be replenished by precipitation due to lower cloud cover. Such mechanisms can explain the marked patterns of concurrent increases in photosynthesis and soil water reduction in densely forested areas shown in Figure 2.

However, the signal in the forests is not uniform globally. The results show a clear dependence on the background climate of the observed responses of ecosystems to water anomalies, consistent with some observations by Madani et al. (2017) and Reich et al. (2018). Light variations exert a dominant control in the tropical regions while temperate forests tend to be more sensitive to water availability than more boreal areas (see Figures S7 and S8 and a detailed discussion in supporting information Text S4; Allen et al., 2010; Angert et al., 2005; Barr et al., 2002; Buermann et al., 2013; Buermann et al., 2018; Ciais et al., 2005; Dass et al., 2016; le Maire et al., 2010; Peng et al., 2011; Piao et al., 2014; Sippel et al., 2017; Trujillo et al., 2012; van Mantgem et al., 2009). Apart from the different sensitivities among forests living in different climates, the observed effect of increased photosynthesis under conditions of decreased soil moisture in general is strongest in colder humid climates (Figures 1 and S7) where water is not the main factor limiting photosynthesis. It poses the question of whether the differential patterns along the tree cover gradient observed in Figure 2 are an artifact of the global distribution of forests, which favors comparatively humid regions, or whether there is an intrinsic interdependence between the amount of trees in an ecosystem and how it responds to variations in soil moisture (De Keersmaecker et al., 2015)? Removing the effect of the mean climate we find that regions with a negative relationship between soil moisture and photosynthetic activity when tree cover is higher (i.e., the higher the tree cover the stronger is the association of lower soil water

content with increased photosynthesis and vice versa, red regions in Figure S9) are larger and more contiguous than areas where the relationship is positive. The occurrence of these regions in all climate zones suggests that it is not the distribution of forests in rather humid climates alone that drives the response of forests to meteorological variations but that the intrinsic structural and physiological differences of trees and grasses contribute to the observed differential responses between them (Sims et al., 2014). The most reasonable explanations for this behavior are the greater rooting depth of trees (Canadell et al., 1996), their water storage capacity in the stems (Matheny et al., 2015), and different strategies of water conservation between grasses and trees (Kelliher et al., 1993; Teuling et al., 2010).

3.3. The Importance of Greenness Versus Photosynthesis to Assess Variability in Ecosystem Productivity

The regular co-occurrence of increased forest photosynthesis at reduced soil water content (and vice versa), as consistently indicated by SIF and model GPP, cannot reliably be identified using satellite observations of EVI (Figures 1 and 2). The negative covariations of light with soil moisture that strongly drive the fluctuations in forest photosynthesis together with temperature when changes in greenness are largely absent (Figure 3a) can explain the different response of EVI (greenness) from SIF and modeled GPP (photosynthesis) in forests. Furthermore, even though there is striking qualitative consistency between GPP and SIF anomalies, GPP patterns appear to be stronger for the same soil moisture and tree cover conditions compared to SIF anomalies (Figure 2). This is not necessarily due to different physiological responses but could be explained by observational issues of SIF and GPP. In fact, SIF observations are only available for low to moderate cloud cover, which limits the range of radiation conditions that they represent. This observation-constrained radiation gradient propagates to attenuated SIF anomalies and contributes to the overall weaker anomaly patterns of SIF compared to GPP. Clearly, larger noise in the SIF observations compared to the empirically modeled GPP could also further dilute the SIF signal. Moreover, GPP data represent model results with inherent uncertainties and such data-driven approaches have known deficiencies to accurately track water stress (Tramontana et al., 2016). Caution is further warranted in the interpretation of the results in Figures 2d–2f because the product of EVI and global radiation does not accurately describe the light energy absorbed by photosynthetically active plant material (green APAR). Still, the observed patterns proved to be replicable with different greenness indices and another data set of SIF (cf. MODIS NDVI, Tucker, 1979; NIRv, Badgley et al., 2017; and NASA SIF, Joiner et al., 2013; Joiner et al., 2016, in Figures S10 and S11). They are also robust with respect to another soil moisture data set used to define meteorological events (ERAInterim and GLEAM; supporting information Figure S12, Martens et al., 2017; Miralles et al., 2011) and across climate zones (supporting information Figure S7). They even hold for some very large soil moisture deviations (Figures 2 and S13).

While the similar patterns of average variability among different Earth observation products of greenness on the one hand, and among various indicators of photosynthesis on the other hand, build confidence in our results, they represent average patterns based on a limited number of occurrences of soil moisture fluctuations of all magnitudes. The enhancement of forest photosynthesis during periods of high radiation and temperature and reduced soil water content, as observed on average in our results, has also been reported for some very extreme events like for the strong drought in temperate forests in the United States in 2012 (Wolf et al., 2016) or forested areas in Russia during the heat wave in 2010 (Flach et al., 2018). Yoshida et al. (2015) found strong reductions in photosynthesis and greenness in grassland and crops during the same event due to heat effects on the canopy structure, while forest greenness shows insignificant changes and absorbed radiation is enhanced in forests—consistent with our observations. We can further confirm their finding that for forests, soil moisture effects appear primarily as changes in photosynthetic LUEf and LUEp. Conversely, they report strong effects of decreased LUEf and LUEp on total negative anomalies in SIF and GPP in forests. In other studies, contradictory responses of forest greenness to reduced soil moisture are reported. Observations range from negative deviations in the absence of structural changes, via no or only small (Sims et al., 2014; Vicca et al., 2016) greenness changes for extreme drought events, to an apparent green-up under conditions of decreased soil water content (Sims et al., 2014) or under extreme heat (Zhang et al., 2015). These inconsistent patterns reinforce the importance of differentiating between greenness and photosynthesis in any kind of ecosystem study, and they highlight the clear need for advanced observational capabilities of the phenomena at large spatial scale. Also, for climate studies it is of key importance to have an observational system that reliably tracks vegetation responses to anomalous environmental conditions. The results of our study suggest that satellite derived SIF may be a valuable asset in such a refined observational system, which

is facilitated by SIF's sensitivity to instantaneous photosynthetic functioning and absorbed light energy by chlorophyll, its direct link to plant chlorophyll content, or both. It demonstrates the capacity to inform on short-term responses of vegetation to meteorological anomalies where traditional greenness observations reach their detection limit that results from the intrinsic difference between photosynthesis and greenness.

4. Conclusions

The main conclusion to take from our study is twofold: (i) The deviations in vegetation greenness and photosynthesis that are associated with times of fluctuating soil moisture differ in sign between ecosystems with higher or lower abundances of trees and (ii) estimates of greenness and photosynthesis show contrasting average responses in regions with higher tree cover. Our results confirm the importance of water for vegetation productivity that has emerged from a large body of literature. Nonwoody semiarid ecosystems strongly respond to the availability of soil water. At the same time, our findings show that—although apparently obvious—any short-term surplus of water will not necessarily be beneficial for photosynthesis everywhere. Specifically, on the time scales of investigation, photosynthesis in ecosystems with more than 50% tree cover is more strongly affected by the covariations in light and temperature than by soil moisture itself, with variations in the degree of its dependencies on the prevailing climate conditions. In contrast to photosynthesis, greenness does barely change in those areas.

These patterns have both ecological and methodological implications. First, the differential relationship of forested and nonforested ecosystems with soil moisture has important consequences for the functioning of ecosystems in regions with extensive ongoing deforestation or afforestation. Man-made changes in forest cover modify the degree to which carbon uptake by vegetation is limited and consequently affected by water or light (or temperature). Also, the related fluxes of energy and water will likely be altered (Duveiller et al., 2018; Forzieri et al., 2017; Teuling et al., 2010). In addition, modifications in vegetation-atmosphere feedbacks might cause fundamental shifts between a possible intensification or a mitigation of meteorological anomalies of all magnitudes, including extremes such as droughts (Green et al., 2017; Miralles et al., 2016; Seneviratne et al., 2010; Zscheischler et al., 2015). Second, we highlight the intrinsic but often neglected crucial difference between plant greenness and photosynthetic activity. In the absence of more direct proxies of productivity, a large part of the available research on ecosystem productivity in relation to environmental factors has relied exclusively on greenness or related variables. This is straightforward in nonwoody vegetation where greenness and photosynthesis often change concomitantly. Clearly, forest photosynthesis often fluctuates in the absence of strong greenness changes. However, greenness variations have been extensively used in the literature to study changes in productivity. This calls for revisiting the conclusions of these studies with proxies closer to photosynthesis, such as SIF.

Acknowledgments
The authors declare no competing financial interest. We thank Michele Meroni and Markus Reichstein for valuable discussion and Ramdane Alkama for processing the Hansen forest cover map. Thanks also to Ulrich Weber for processing CERES data. S. W. and L. G. were funded by the Emmy Noether Programme of the German Research Foundation (GU 1276/1-1). S. W. acknowledges financial support through a scholarship from the German Academic Exchange Service (DAAD). M. J. acknowledges support from the EU H2020 BACI project (grant 640176). S. W. is also supported by the European Union's Horizon 2020 research and innovation program under grant agreement 776186 (CHE project) and agreement 776810 (VERIFY project). G. C.-V. work has been supported by EU under the ERC consolidator grant SEDAL-647423. Data supporting the conclusions of this study are properly cited and publicly available. SIF GFZ data have been retrieved from ftp://ftp.gfz-potsdam.de/home/mefe/GlobFluo/GOME-2/ungridded/ and SIF NASA v26 from https://avdc.gsfc.nasa.gov/pub/data/satellite/MetOp/GOME_F/. MODIS MCD43C4v005 data were retrieved from the online Reverb, courtesy of the NASA EOSDIS Land Processes Distributed Active Archive Center (LP DAAC), USGS/Earth Resources Observation and Science (EROS) Center, Sioux Falls, South Dakota, https://lpdaac.usgs.gov/dataset_discovery/modis/modis_products_table/mcd43c4. FLUXCOM-RS model GPP is available at ftp://ftp.bgc-jena.mpg.de/pub/outgoing/FluxCom/CarbonFluxes/RS/ensemble/4320_2160/8daily/. Meteorological data can be downloaded from ECMWF ERA-Interim reanalysis, http://apps.ecmwf.int/datasets/data/interim-full-daily/levtype=sfc/, and soil moisture model data from the GLEAM project from https://www.gleam.eu/, both after registration. CERES SYN1deg-Day product has been obtained from https://ceres-tool.larc.nasa.gov/ord-tool/jsp/SYN1degEd4Selection.jsp. Current Koeppen-Geiger climate classification is published under http://koeppen-geiger.vu-wien.ac.at/present.htm and global forest cover (change) under http://earthenginepartners.appspot.com/science-2013-global-forest/download_v1.5.html.

References

Ahlström, A., Raupach, M. R., Schurgers, G., Smith, B., Arneth, A., Jung, M., et al. (2015). The dominant role of semi-arid ecosystems in the trend and variability of the land CO_2 sink. *Science*, *348*(6237), 895–899. https://doi.org/10.1126/science.aaa1668

Allen, C. D., Macalady, A. K., Chenchouni, H., Bachelet, D., McDowell, N., Vennetier, M., et al. (2010). A global overview of drought and heat-induced tree mortality reveals emerging climate change risks for forests. *Forest Ecology and Management*, *259*(4), 660–684. https://doi.org/10.1016/j.foreco.2009.09.001

Angert, A., Biraud, S., Bonfils, C., Henning, C. C., Buermann, W., Pinzon, J., et al. (2005). Drier summers cancel out the CO_2 uptake enhancement induced by warmer springs. *Proceedings of the National Academy of Sciences of the United States of America*, *102*(31), 10,823–10,827. https://doi.org/10.1073/pnas.0501647102

Asner, G. P., & Alencar, A. (2010). Drought impacts on the Amazon forest: The remote sensing perspective. *New Phytologist*, *187*(3), 569–578. https://doi.org/10.1111/j.1469-8137.2010.03310.x

Badgley, G., Field, C. B., & Berry, J. A. (2017). Canopy near-infrared reflectance and terrestrial photosynthesis. *Science Advances*, *3*(3), e1602244. https://doi.org/10.1126/sciadv.1602244

Barber, V. A., Juday, G. P., & Finney, B. P. (2000). Reduced growth of alaskan white spruce in the twentieth century from temperature-induced drought stress. *Nature*, *405*, 319–326.

Barr, A. G., Griffis, T. J., Black, T. A., Lee, X., Staebler, R. M., Fuentes, J. D., et al. (2002). Comparing the carbon budgets of boreal and temperate deciduous forest stands. *Canadian Journal of Forest Research*, *32*(5), 813–822. https://doi.org/10.1139/x01-131

Baumbach, L., Siegmund, J. F., Mittermeier, M., & Donner, R. V. (2017). Impacts of temperature extremes on European vegetation during the growing season. *Biogeosciences*, *14*(21), 4891–4903. https://doi.org/10.5194/bg-14-4891-2017

Beer, C., Reichstein, M., Tomelleri, E., Ciais, P., Jung, M., Carvalhais, N., et al. (2010). Terrestrial gross carbon dioxide uptake: Global distribution and covariation with climate. *Science*, *329*(5993), 834–838. https://doi.org/10.1126/science.1184984

Brando, P. M., Goetz, S. J., Baccini, A., Nepstad, D. C., Beck, P. S. A., & Christman, M. C. (2010). Seasonal and interannual variability of climate and vegetation indices across the Amazon. *Proceedings of the National Academy of Sciences*, *107*(33), 14,685–14,690. https://doi.org/10.1073/pnas.0908741107

Braswell, B. H., Schimel, D. S., Linder, E., & Moore, B. (1997). The response of global terrestrial ecosystems to interannual temperature variability. *Science*, *278*(5339), 870–873. https://doi.org/10.1126/science.278.5339.870

Buermann, W., Forkel, M., O'Sullivan, M., Sitch, S., Friedlingstein, P., Haverd, V., et al. (2018). Widespread seasonal compensation effects of spring warming on northern plant productivity. *Nature*, *562*(7725), 110–114. https://doi.org/10.1038/s41586-018-0555-7

Buermann, W., Parida, R. B., Jung, M., Burn, D. H., & Reichstein, M. (2013). Earlier springs decrease peak summer productivity in North American boreal forests. *Environmental Research Letters*, *8*(2), 024027.

Canadell, J., Jackson, R. B., Ehleringer, J. B., Mooney, H. A., Sala, O. E., & Schulze, E. D. (1996). Maximum rooting depth of vegetation types at the global scale. *Oecologia*, *108*(4), 583–595. https://doi.org/10.1007/BF00329030

Ceccherini, G., Gobron, N., & Migliavacca, M. (2014). On the response of european vegetation phenology to hydroclimatic anomalies. *Remote Sensing*, *6*(4), 3143–3169. https://doi.org/10.3390/rs6043143

Ciais, P., Reichstein, M., Viovy, N., Granier, A., Oge, J., Allard, V., et al. (2005). Europe-wide reduction in primary productivity caused by the heat and drought in 2003. *Nature Letters*, *437*, 529–533. https://doi.org/10.1038/nature03972

Dass, P., Rawlins, M. A., Kimball, J. S., & Kim, Y. (2016). Environmental controls on the increasing GPP of terrestrial vegetation across northern Eurasia. *Biogeosciences*, *13*(1), 45–62. https://doi.org/10.5194/bg-13-45-2016

De Keersmaecker, W., Lhermitte, S., Tits, L., Honnay, O., Somers, B., & Coppin, P. (2015). A model quantifying global vegetation resistance and resilience to short-term climate anomalies and their relationship with vegetation cover. *Global Ecology and Biogeography*, *24*(5), 539–548. https://doi.org/10.1111/geb.12279

Dee, D. P., Uppala, S. M., Simmons, A. J., Berrisford, P., Poli, P., Kobayashi, S., et al. (2011). The ERA-Interim reanalysis: Configuration and performance of the data assimilation system. *Quarterly Journal of the Royal Meteorological Society*, *137*(656), 553–597. https://doi.org/10.1002/qj.828

Doelling, D. R., Loeb, N. G., Keyes, D. F., Nordeen, M. L., Morstad, D., Nguyen, C., et al. (2013). Geostationary enhanced temporal interpolation for ceres flux products. *Journal of Atmospheric and Oceanic Technology*, *30*(6), 1072–1090. https://doi.org/10.1175/JTECH-D-12-00136.1

Donges, J., Schleussner, C. F., Siegmund, J., & Donner, R. (2016). Event coincidence analysis for quantifying statistical interrelationships between event time series. *The European Physical Journal Special Topics*, *225*(3), 471–487. https://doi.org/10.1140/epjst/e2015-50233-y

Duveiller, G., Hooker, J., & Cescatti, A. (2018). The mark of vegetation change on Earth's surface energy balance. *Nature Communications*, *9*, 679. https://doi.org/10.1038/s41467-017-02810-8

Fisher, J. B., Melton, F., Middleton, E., Hain, C., Anderson, M., Allen, R., et al. (2017). The future of evapotranspiration: Global requirements for ecosystem functioning, carbon and climate feedbacks, agricultural management, and water resources. *Water Resources Research*, *53*, 2618–2626. https://doi.org/10.1002/2016WR020175

Flach, M., Sippel, S., Gans, F., Bastos, A., Brenning, A., Reichstein, M., & Mahecha, M. D. (2018). Contrasting biosphere responses to hydrometeorological extremes: Revisiting the 2010 western Russian Heatwave. *Biogeosciences Discussions*, *2018*, 1–21. https://doi.org/10.5194/bg-2018-130

Forzieri, G., Alkama, R., Miralles, D. G., & Cescatti, A. (2017). Satellites reveal contrasting responses of regional climate to the widespread greening of Earth. *Science*, *356*(6343), 1180–1184. https://doi.org/https://doi.org/10.1126/science.aal1727

Frank, D., Reichstein, M., Bahn, M., Thonicke, K., Frank, D., Mahecha, M. D., et al. (2015). Effects of climate extremes on the terrestrial carbon cycle: Concepts, processes and potential future impacts. *Global Change Biology*, *21*(8), 2861–2880. https://doi.org/10.1111/gcb.12916

Frankenberg, C., Fisher, J. B., Worden, J., Badgley, G., Saatchi, S. S., Lee, J. E., et al. (2011). New global observations of the terrestrial carbon cycle from GOSAT: Patterns of plant fluorescence with gross primary productivity. *Geophysical Research Letters*, *38*, L17706. https://doi.org/10.1029/2011GL048738

Green, J. K., Konings, A. G., Alemohammad, S. H., Berry, J., Entekhabi, D., Kolassa, J., et al. (2017). Regionally strong feedbacks between the atmosphere and terrestrial biosphere. *Nature Geoscience*, *10*, 410–414. https://doi.org/10.1038/ngeo2957

Guan, K., Pan, m., Li, H., Wolf, A., Wu, J., Medvigy, D., et al. (2015). Photosynthetic seasonality of global tropical forests constrained by hydroclimate. *Nature Geoscience*, *8*, 284–289. https://doi.org/10.1038/NGEO2382

Hansen, M. C., Potapov, P. V., Moore, R., Hancher, M., Turubanova, S. A., Tyukavina, A., et al. (2013). High-resolution global maps of 21st-century forest cover change. *Science*, *342*(6160), 850–853. https://doi.org/10.1126/science.1244693

Huang, L., He, B., Chen, A., Wang, H., Liu, J., Lü, A., & Chen, Z. (2016). Drought dominates the interannual variability in global terrestrial net primary production by controlling semi-arid ecosystems. *Scientific Reports*, *6*, 24639. https://doi.org/10.1038/srep24639

Huete, A., Didan, K., Miura, T., Rodriguez, E. P., Gao, X., & Ferreira, L. G. (2002). Overview of the radiometric and biophysical performance of the MODIS vegetation indices. *Remote Sensing of Environment*, *83*, 195–213. PII: S0034-4257(02)00096-2.

Huete, A., Didan, K., Shimabukuro, Y. E., Ratana, P., Saleska, S. R., Hutyra, L. R., et al. (2006). Amazon rainforests greenup with sunlight in dry season. *Geophysical Research Letters*, *33*, L06405. https://doi.org/10.1029/2005GL025583

Joiner, J., Guanter, L., Lindstrot, R., Voigt, M., Vasilkov, A. P., Middleton, E. M., et al. (2013). Global monitoring of terrestrial chlorophyll fluorescence from moderate-spectral-resolution near-infrared satellite measurements: Methodology, simulations, and application to GOME-2. *Atmospheric Measurement Techniques*, *6*(10), 2803–2823. https://doi.org/10.5194/amt-6-2803-2013

Joiner, J., Yoshida, Y., Guanter, L., & Middleton, E. M. (2016). New methods for the retrieval of chlorophyll red fluorescence from hyperspectral satellite instruments: Simulations and application to GOME-2 and SCIAMACHY. *Atmospheric Measurement Techniques*, *9*(8), 3939–3967. https://doi.org/10.5194/amt-9-3939-2016

Joiner, J., Yoshida, Y., Vasilkov, A. P., Yoshida, Y., Corp, L. A., & Middleton, E. M. (2011). First observations of global and seasonal terrestrial chlorophyll fluorescence from space. *Biogeosciences*, *8*(3), 637–651. https://doi.org/10.5194/bg-8-637-2011

Jung, M., Reichstein, M., Margolis, H. A., Cescatti, A., Richardson, A. D., Arain, M. A., et al. (2011). Global patterns of land-atmosphere fluxes of carbon dioxide, latent heat, and sensible heat derived from eddy covariance, satellite, and meteorological observations. *Journal of Geophysical Research*, *116*, G00J07. https://doi.org/10.1029/2010JG001566

Jung, M., Reichstein, M., Schwalm, C. R., Huntingford, C., Sitch, S., Ahlström, A., et al. (2017). Compensatory water effects link yearly global land CO_2 sink changes to temperature. *Nature*, *541*, 516–520. https://doi.org/10.1038/nature20780

Kelliher, F. M., Leuning, R., & Schulze, E. D. (1993). Evaporation and canopy characteristics of coniferous forests and grasslands. *Oecologia*, *95*(2), 153–163. https://doi.org/10.1007/BF00323485

Köhler, P., Guanter, L., & Joiner, J. (2015). A linear method for the retrieval of sun-induced chlorophyll fluorescence from GOME-2 and SCIAMACHY data. *Atmospheric Measurement Techniques*, *8*(6), 2589–2608. https://doi.org/10.5194/amt-8-2589-2015

Koirala, S., Jung, M., Reichstein, M., de Graaf, I. E. M., Camps-Valls, G., Ichii, K., et al. (2017). Global distribution of groundwater-vegetation spatial covariation. *Geophysical Research Letters*, *44*, 4134–4142. https://doi.org/10.1002/2017GL072885

Koster, R. D., Dirmeyer, P. A., Guo, Z., Bonan, G., Chan, E., Cox, P., et al. (2004). Regions of strong coupling between soil moisture and precipitation. *Science*, *305*(5687), 1138–1140. https://doi.org/10.1126/science.1100217

Kottek, M., Grieser, J., Beck, C., Rudolf, B., & Rubel, F. (2006). World Map of the Köppen-Geiger climate classification updated. *Meteorologische Zeitschrift*, *15*(3), 259–263. https://doi.org/10.1127/0941-2948/2006/0130

le Maire, G., Delpierre, N., Jung, M., Ciais, P., Reichstein, M., Viovy, N., et al. (2010). Detecting the critical periods that underpin interannual fluctuations in the carbon balance of European forests. *Journal of Geophysical Research*, *115*, G00H03. https://doi.org/10.1029/2009JG001244

Liu, J., Bowman, K., Schimel, D., Parazoo, N., Jiang, Z., Lee, M., et al. (2017). Contrasting carbon cycle responses of the tropical continents to the 2015–2016 El Niño. *Science*, *358*, 6360. https://doi.org/10.1126/science.aam5690

Liu, G., Liu, H., & Yin, Y. (2013). Global patterns of NDVI-indicated vegetation extremes and their sensitivity to climate extremes. *Environmental Research Letters*, *8*(2), 025009.

Lyapustin, A., Wang, Y., Xiong, X., Meister, G., Platnick, S., Levy, R., et al. (2014). Scientific impact of MODIS C5 calibration degradation and C6+ improvements. *Atmospheric Measurement Techniques*, *7*(12), 4353–4365. https://doi.org/10.5194/amt-7-4353-2014

Madani, N., Kimball, J., Jones, L., Parazoo, N., & Guan, K. (2017). Global analysis of bioclimatic controls on ecosystem productivity using satellite observations of solar-induced chlorophyll fluorescence. *Remote Sensing*, *9*(6), 530. https://doi.org/10.3390/rs9060530

Mahecha, M. D., Gans, F., Sippel, S., Donges, J. F., Kaminski, T., Metzger, S., et al. (2017). Detecting impacts of extreme events with ecological in situ monitoring networks. *Biogeosciences*, *14*(18), 4255–4277. https://doi.org/10.5194/bg-14-4255-2017

Martens, B., Miralles, D. G., Lievens, H., van der Schalie, R., de Jeu, R. A. M., Fernández-Prieto, D., et al. (2017). GLEAM v3: Satellite-based land evaporation and root-zone soil moisture. *Geoscientific Model Development*, *10*(5), 1903–1925. https://doi.org/10.5194/gmd-10-1903-2017

Matheny, A. M., Bohrer, G., Garrity, S. R., Morin, T. H., Howard, C. J., & Vogel, C. S. (2015). Observations of stem water storage in trees of opposing hydraulic strategies. *Ecosphere*, *6*(9), 1–13. https://doi.org/10.1890/ES15-00170.1

Meroni, M., Rossini, M., Guanter, L., Alonso, L., Rascher, U., Colombo, R., & Moreno, J. (2009). Remote sensing of solar-induced chlorophyll fluorescence: Review of methods and applications. *Remote Sensing of Environment*, *113*(10), 2037–2051. https://doi.org/https://doi.org/10.1016/j.rse.2009.05.003

Miralles, D., Holmes, T., De Jeu, R., Gash, J., Meesters, A., & Dolman, A. (2011). Global land-surface evaporation estimated from satellite-based observations. *Hydrology and Earth System Sciences*, *15*(2), 453–469. https://doi.org/10.5194/hess-15-453-2011

Miralles, D., Nieto, R., McDowell, N., Dorigo, W., Verhoest, N., Liu, Y., et al. (2016). Contribution of water-limited ecoregions to their own supply of rainfall. *Environmental Research Letters*, *11*(12), 124007. http://stacks.iop.org/1748-9326/11/i=12/a=124007

Monteith, J. L. (1972). Solar radiation and productivity in tropical ecosystems. *Journal of Applied Ecology*, *9*(3), 747–766.

Moore, C. E., Brown, T., Keenan, T. F., Duursma, R. A., van Dijk, A. I. J. M., Beringer, J., et al. (2016). Reviews and syntheses: Australian vegetation phenology: New insights from satellite remote sensing and digital repeat photography. *Biogeosciences*, *13*(17), 5085–5102. https://doi.org/10.5194/bg-13-5085-2016

Morton, D. C., Nagol, J., Carabajal, C. C., Rosette, J., Palace, M., Cook, B. D., et al. (2014). Amazon forests maintain consistent canopy structure and greenness during the dry season. *Nature*, *506*, 221–224. https://doi.org/10.1038/nature13006

Myneni, R. B., Yang, W., Nemani, R. R., Huete, A. R., Dickinson, R. E., Knyazikhin, Y., et al. (2007). Large seasonal swings in leaf area of Amazon rainforests. *Proceedings of the National Academy of Sciences*, *104*(12), 4820–4823. https://doi.org/10.1073/pnas.0611338104

Nemani, R. R., Keeling, C. D., Hashimoto, H., Jolly, W. M., Piper, S. C., Tucker, C. J., et al. (2003). Climate-driven increases in global terrestrial net primary production from 1982 to 1999. *Science*, *300*, 1560–1563. https://doi.org/10.1126/science.1082750

Peng, C., Ma, Z., Lei, X., Zhu, Q., Chen, H., Wang, W., et al. (2011). A drought-induced pervasive increase in tree mortality across Canada's boreal forests. *Nature Climate Change*, *1*, 467–471. https://doi.org/10.1038/nclimate1293

Piao, S., Nan, H., Huntingford, C., Ciais, P., Friedlingstein, P., Sitch, S., et al. (2014). Evidence for a weakening relationship between interannual temperature variability and northern vegetation activity. *Nature Communications*, *5*, 5018. https://doi.org/10.1038/ncomms6018

Porcar-Castell, A., Tyystjärvi, E., Atherton, J., van der Tol, C., Flexas, J., Pfündel, E. E., et al. (2014). Linking chlorophyll a fluorescence to photosynthesis for remote sensing applications: Mechanisms and challenges. *Journal of Experimental Botany*, *65*(15), 4065–4095. https://doi.org/10.1093/jxb/eru191

Poulter, B., Frank, D., Ciais, P., Myneni, R. B., Andela, N., Bi, J., et al. (2014). Contribution of semi-arid ecosystems to interannual variability of the global carbon cycle. *Nature*, *509*, 600–603. https://doi.org/10.1038/nature13376

Rammig, A., Wiedermann, M., Donges, J. F., Babst, F., von Bloh, W., Frank, D., et al. (2015). Coincidences of climate extremes and anomalous vegetation responses: Comparing tree ring patterns to simulated productivity. *Biogeosciences*, *12*(2), 373–385. https://doi.org/10.5194/bg-12-373-2015

Reich, P. B., Sendall, K. M., Stefanski, A., Rich, R. L., Hobbie, S. E., & Montgomery, R. A. (2018). Effects of climate warming on photosynthesis in boreal tree species depend on soil moisture. *Nature*, *562*, 263–267. https://doi.org/10.1038/s41586-018-0582-4

Reichstein, M., Bahn, M., Ciais, P., Frank, D., Mahecha, M. D., Seneviratne, S. I., et al. (2013). Climate extremes and the carbon cycle. *Nature*, *500*(7462), 287–295. https://doi.org/10.1038/nature12350

Rubel, F., Brugger, K., Haslinger, K., & Auer, I. (2017). The climate of the European Alps: Shift of very high resolution Kppen-Geiger climate zones 1800–2100. *Meteorologische Zeitschrift*, *26*(2), 115–125. https://doi.org/10.1127/metz/2016/0816

Saleska, S. R., Didan, K., Huete, A. R., & da Rocha, H. R. (2007). Amazon forests green-up during 2005 drought. *Science*, *318*(5850), 612–612. https://doi.org/10.1126/science.1146663

Schimel, D., Pavlick, R., Fisher, J. B., Asner, G. P., Saatchi, S., Townsend, P., et al. (2015). Observing terrestrial ecosystems and the carbon cycle from space. *Global Change Biology*, *21*(5), 1762–1776. https://doi.org/10.1111/gcb.12822

Schwalm, C. R., Williams, C. A., Schaefer, K., Baldocchi, D., Black, T. A., Goldstein, A. H., et al. (2012). Reduction in carbon uptake during turn of the century drought in western North America. *Nature Geoscience*, *5*, 551–556. https://doi.org/10.1038/ngeo1529

Seneviratne, S. I., Corti, T., Davin, E. L., Hirschi, M., Jaeger, E. B., Lehner, I., et al. (2010). Investigating soil moisture-climate interactions in a changing climate: A review. *Earth-Science Reviews*, *99*(3–4), 125–161. https://doi.org/10.1016/j.earscirev.2010.02.004

Sims, D. A., Brzostek, E. R., Rahman, A., Dragoni, D., & Phillips, R. P. (2014). An improved approach for remotely sensing water stress impacts on forest C uptake. *Global Change Biology*, *20*(9), 2856–2866. https://doi.org/10.1111/gcb.12537

Sippel, S., Forkel, M., Rammig, A., Thonicke, K., Flach, M., Heimann, M., et al. (2017). Contrasting and interacting changes in simulated spring and summer carbon cycle extremes in European ecosystems. *Environmental Research Letters*, *12*, 075006. https://doi.org/10.1088/1748-9326/aa7398

Smith, M. D. (2011). An ecological perspective on extreme climatic events: A synthetic definition and framework to guide future research. *Journal of Ecology*, *99*(3), 656–663. https://doi.org/10.1111/j.1365-2745.2011.01798.x

Sun, Y., Fu, R., Dickinson, R., Joiner, J., Frankenberg, C., Gu, L., et al. (2015). Drought onset mechanisms revealed by satellite solar-induced chlorophyll fluorescence: Insights from two contrasting extreme events. *Journal of Geophysical Research: Biogeosciences*, *120*, 2427–2440. https://doi.org/10.1002/2015JG003150

Teuling, A. J., Seneviratne, S. I., Stöckli, R., Reichstein, M., Moors, E., Ciais, P., et al. (2010). Contrasting response of European forest and grassland energy exchange to heatwaves. *Nature Geoscience*, *3*, 722–727. https://doi.org/10.1038/ngeo950

Tramontana, G., Jung, M., Schwalm, C. R., Ichii, K., Camps-Valls, G., Ráduly, B., et al. (2016). Predicting carbon dioxide and energy fluxes across global FLUXNET sites with regression algorithms. *Biogeosciences*, *13*(14), 4291–4313. https://doi.org/10.5194/bg-13-4291-2016

Trujillo, E., Molotch, N. P., Goulden, M. L., Kelly, A. E., & Bales, R. C. (2012). Elevation-dependent influence of snow accumulation on forest greening. *Nature Geoscience*, *5*, 705–709. https://doi.org/10.1038/ngeo1571

Tucker, C. J. (1979). Red and photographic infrared linear combinations for monitoring vegetation. *Remote sensing of Environment*, *8*(2), 127–150.

van Mantgem, P. J., Stephenson, N. L., Byrne, J. C., Daniels, L. D., Franklin, J. F., Fulé, P. Z., et al. (2009). Widespread increase of tree mortality rates in the western United States. *Science*, *323*(5913), 521–524. https://doi.org/10.1126/science.1165000

van der Molen, M. K., Dolman, A. J., Ciais, P., Eglin, T., Gobron, N., Law, B. E., et al. (2011). Drought and ecosystem carbon cycling. *Agricultural and Forest Meteorology*, *151*(7), 765–773. https://doi.org/10.1016/j.agrformet.2011.01.018

Vicca, S., Balzarolo, M., Filella, I., Granier, A., Herbst, M., Knohl, A., et al. (2016). Remotely-sensed detection of effects of extreme droughts on gross primary production. *Scientific Reports*, *6*, 28269. https://doi.org/10.1038/srep28269

Vicente-Serrano, S. M., Gouveia, C., Camarero, J. J., Beguería, S., Trigo, R., López-Moreno, J. I., et al. (2013). Response of vegetation to drought time-scales across global land biomes. *Proceedings of the National Academy of Sciences of the United States of America*, *110*(1), 52–57. http://doi.org/10.1073/pnas.1207068110

Wolf, S., Keenan, T. F., Fisher, J. B., Baldocchi, D. D., Desaie, A. R., Richardson, A. D., et al. (2016). Warm spring reduced carbon cycle impact of the 2012 US summer drought. *Proceedings of the National Academy of Sciences of the United States of America*, *113*, 1–6. https://doi.org/10.1073/pnas.1519620113

Wu, J., Kobayashi, H., Stark, S. C., Meng, R., Guan, K., Nguyen Tran, N., et al. (2018). Biological processes dominate seasonality of remotely sensed canopy greenness in an Amazon evergreen forest. *New Phytologist*, *217*(4), 1507–1520. https://doi.org/10.1111/nph.14939

Wu, J., van der Linden, L., Lasslop, G., Carvalhais, N., Pilegaard, K., Beier, C., & Ibrom, A. (2012). Effects of climate variability and functional changes on the interannual variation of the carbon balance in a temperate deciduous forest. *Biogeosciences*, *9*(1), 13–28. https://doi.org/10.5194/bg-9-13-2012

Yoshida, Y., Joiner, J., Tucker, C., Berry, J., Lee, J. E., Walker, G., et al. (2015). The 2010 Russian drought impact on satellite measurements of solar-induced chlorophyll fluorescence: Insights from modeling and comparisons with parameters derived from satellite reflectances. *Remote Sensing of Environment*, *166*(0), 163–177. https://doi.org/10.1016/j.rse.2015.06.008

Zarco-Tejada, P. J., Morales, A., Testi, L., & Villalobos, F. J. (2013). Spatio-temporal patterns of chlorophyll fluorescence and physiological and structural indices acquired from hyperspectral imagery as compared with carbon fluxes measured with eddy covariance. *Remote Sensing of Environment*, *133*, 102–115. https://doi.org/https://doi.org/10.1016/j.rse.2013.02.003

Zhang, Y., Voigt, M., & Liu, H. (2015). Contrasting responses of terrestrial ecosystem production to hot temperature extreme regimes between grassland and forest. *Biogeosciences*, *12*(2), 549–556. https://doi.org/10.5194/bg-12-549-2015

Zhang, Y., Xiao, X., Zhou, S., Ciais, P., McCarthy, H., & Luo, Y. (2016). Canopy and physiological control of GPP during drought and heatwave. *Geophysical Research Letters*, *43*, 3325–3333. https://doi.org/10.1002/2016GL068501

Zhang, Y., Zhu, Z., Liu, Z., Zeng, Z., Ciais, P., Huang, M., et al. (2016). Seasonal and interannual changes in vegetation activity of tropical forests in Southeast Asia. *Agricultural and Forest Meteorology*, *224*, 1–10. https://doi.org/10.1016/j.agrformet.2016.04.009

Zhao, M., & Running, S. (2010). Drought-induced reduction in global terrestrial net primary production from 2000 through 2009. *Science*, *329*(5994), 940–943. https://doi.org/10.1126/science.1192666

Zhou, S., Zhang, Y., Caylor, K. K., Luo, Y., Xiao, X., Ciais, P., et al. (2016). Explaining inter-annual variability of gross primary productivity from plant phenology and physiology. *Agricultural and Forest Meteorology*, *226-227*, 246–256. https://doi.org/https://doi.org/10.1016/j.agrformet.2016.06.010

Zscheischler, J., Mahecha, M. D., Harmeling, S., & Reichstein, M. (2013). Detection and attribution of large spatiotemporal extreme events in earth observation data. *Ecological Informatics*, *15*, 66–73. http://dx.do.org/10.1016/j.ecoinf.2013.03.004

Zscheischler, J., Orth, R., & Seneviratne, S. I. (2015). A submonthly database for detecting changes in vegetation-atmosphere coupling. *Geophysical Research Letters*, *42*, 9816–9824. https://doi.org/10.1002/2015GL066563

Zscheischler, J., Reichstein, M., Harmeling, S., Rammig, A., Tomelleri, E., & Mahecha, M. D. (2014). Extreme events in gross primary production: A characterization across continents. *Biogeosciences*, *11*(11), 2909–2924. https://doi.org/10.5194/bg-11-2909-2014